

Numerical Study of Stress Concentration in a Tensioned Plate

Dr.Riyah N.Kiter
Assistant Professor

Ahmed N.Uwayed
Assistant Teacher
University of Anbar

Arz Yahya Rzayyig
Assistant Teacher

Abstract

A numerical study using (FEM) has been carried out to investigate the effect of some parameters on the stress concentration factor in a plate, having different types of cutout and subjected to uniaxial tension. These parameters include the location of cutout, orientation of cutout with respect to the axis of loading, radius of bluntness of cutout and the thickness of the plate. Maximum values of stress concentration factor (SCF) were found in cases of: 1. the cutout is in the center of the plate, 2. the angle of a corner of cutout is bisected by an axis perpendicular to the loading axis, 3. the corners of cutout are sharp (zero radius), and 4.the plate is very thin.

Keywords: Plates, Cutouts, Concentration factors, Finite element, Tensile.

دراسة عددية لتمرکز الإجهاد في صفيحة مشدودة

الخلاصة:

أجريت دراسة عددية باستخدام طريقة العناصر المحددة لغرض البحث في تأثير بعض العوامل على معامل تمرکز الأجهاد في صفيحة تحتوي على قطوعات مختلفة و معرضة لشد محوري احادي. تضمنت هذه العوامل موقع القطع ، اتجاه القطع بالنسبة لمحور التحميل ، نصف قطر حافة القطع و سمك الصفيحة. أظهرت الدراسة ان معامل تمرکز الأجهاد يبلغ ذروته في الحالات التالية : عندما يكون القطع في مركز الصفيحة. عندما تكون زاوية حافة القطع منصفة بمحور عمودي عاى محور التحميل. عندما تكون حافات القطع حادة (نصف قطر يساوي صفر) و أخيراً. عندما تكون الصفيحة رقيقة جداً.

الكلمات الدالة: صفائح، تقوب، معاملات التمرکز، العناصر المحددة، الشد.

Introduction

Plates of various constructions find wide uses as primary structural elements in both modern and classical structures. In recent years, the increasing need of lightweight efficient structures has led the structural engineer to the field of structural shape optimization. Different cutout shapes in structural elements are needed to reduce the weight of the system and provide access to other parts of the structure. It

is well known that the presence of a cutout or hole in a stressed member creates highly localized stresses at the vicinity of the cutout. The ratio of the maximum stress at the cutout edge to the nominal stress is called the stress concentration factor (SCF).

Monahan et al. ^[1] applied the finite element on a clamped rectangular plate with a rectangular hole and verified the numerical results by experiments. Paramasivam ^[2] used the

finite difference method for a simply – supported and clamped rectangular plate with a rectangular hole. Aksu and Ali ^[3] also used the finite element method to analyze a rectangular plate with more than two holes. Rajamani and Prabhakaran ^[4] assumed the effect of the hole is equivalent to an externally applied loading and carried out a numerical analysis based on this assumption for a composite plate.

Rezaepazhand and Jafari^[5] investigated analytically the stress analysis of plates with different central cutouts in an infinite plate under uniaxial tension. The analysis included the effect of cutout shape, bluntness, and orientation on the stress concentration factor.

Rajab^[6] studied the effect of single and multiple notches and holes on the stress concentration factor. Rectangular plates having triangular, square and hexagonal cutouts were loaded in tension, and the stress concentration factor was determined using photoelasticity and finite element techniques.

Lam et al.^[7] divided the rectangular plate with a hole into several subareas and applied the modified (RRM). Lam and Hung ^[8] applied the same method on a stiffened plate. The admissible functions used in Refs.^[7,8] are the orthogonal polynomials proposed by Bhat ^[9-10]. Laura et al. ^[11] calculated the natural vibration characteristic of a simply - supported rectangular plate with a rectangular hole by the classical (RRM). Sakiyama et al. ^[12] analyzed the natural vibration characteristic of orthotropic plate with a square hole by means of the Green function assuming the hole as an extremely thin plate. The vibration analysis of a rectangular plate with a circular hole does not lend an easy approach since the geometry of the hole is not the same as the geometry of the rectangular plate. Takahashi ^[13] used the

classical (RRM) after deriving the total energy by subtracting the energy of the hole from the energy of the whole plate.

Theocaris and Petrou ^[14] used Schwarz –Christoffel transformation to evaluate the stress concentration factor for an infinite plate with central triangular cutout. Stress and strain distributions along the border of rectangular cutout in an infinite elastic plate were presented by Theocaris and Petrou^[15]. Lasko et al.^[16] used relaxation element method to determine the stress fields in a plate with three circular cutouts. Ultimate strength of metallic plates with central circular cutout under shear loading was investigated by Paik ^[17].

Ulza and Semercigilb ^[18] used standard finite elements to present numerical modeling of dynamic behavior of perforated plates. They explored the possibility of employing the cutout as a vibration absorber for controlling the vibration of plates. Effect of electromechanical coupling on stress concentration factors of perforated isotropic piezoelectric materials was presented by Dai et al. ^[19].

Rezaepazhand and Jafari ^[20] investigated stress analysis of composite plates with noncircular cutout subjected to bending load. Furthermore, the effect of cutout shape and load direction on maximum stresses of perforated composite plates with quasi – square cutout was presented.

Despite the importance of SCF in cutouts, little attention has been paid to stress concentration factor in plates with special shaped cutouts. It would be thus of interest to investigate SCF in more general and practical cutouts.

The present work focuses on the effect of cutout type, cutout location, cutout rotation, cutout bluntness and plate thickness on stress concentration factor.

Theoretical Considerations

The uniform distribution of stresses in sections loaded with tension or compression, can be found only in the areas which are somewhat far from the influence of loads assuming that the dimensions are fixed or changing gradually. If the dimensions change dramatically, the distribution of stresses in the cross-section is non uniform^[21]. The phenomenon of sharp increase in stress in these places is called a stress-concentration and stresses in places of concentration can be determined experimentally or using the method of the theory of elasticity. The theoretical stress concentration factor, which is symbolized by K_t is the proportion of the greatest stress to the nominal stress.

$$K_t = \sigma_{\text{Maximum}} / \sigma_{\text{Nominal}} \dots\dots\dots(1)$$

Nominal stress means the stress which is determined by the usual strength of materials without taking into account the effect of concentration, and the theoretical stress-concentration factor K_t , which is determined on the assumption that the material follows Hook's law, does not give the actual effect of concentration of stress on strength of the part in many cases^[21,22]. If the material follows Hook's law before failure, the strength of the part with stresses concentrated will be less than that of no concentration of stress by K_t times. This decrease is determined experimentally by the ratio of the endurance limit (σ_E) of the part without stress concentrations to the endurance of the part including the centralized stress (σ_{EC}).

$$K_f = \sigma_E / \sigma_{EC} \dots\dots\dots(2)$$

K_f is known as the fatigue stress concentration factor. Therefore, experiments showed that in static loading, especially for plastic elements $K_f = 1$ and this means that the stress

concentration is taken into consideration only for parts made of brittle materials or materials of limited plasticity and on impact loading, the stress concentration is taken into account for all materials^[21].

The abrupt changes in the sections has a special significance in the design of machine parts machines which are subjected to external forces and dynamic stresses, where the stress exceeds at some points of change in the section the average stress, and if there is a variable stress it is probable to initiate cracking at these points. Note that most of the failures are attributable to this kind of cracks^[22].

Designers often ignore the concentration of stress, but they reduce the error arising from this ignorance by using high values of safety factor when analyzing the stresses, although this does not justify the ignorance of concentration of stress in cases in which it plays an important role. To understand the mechanism of concentration of stresses assume the strip shown in Fig.(1A), then the tensile stress of a non-perforated strip is:

$$\sigma_{nom} = \frac{F}{A} = \frac{F}{(b.t)} \dots\dots\dots(3)$$

In the perforated strip with a central hole of diameter (d), Fig.(1B), away from the hole the stress remains uniform across the section at σ_{nom} whereas the value of the nominal stress through the hole is $\sigma = F / [(d-b)t]$, and it is uniform at points far from the edge of the hole. The stress at the edge of the hole is in fact greater than this value. Therefore, if the factor of safety is less than the stress concentration factor K_t the engineering part will fail, hence it is necessary not to rely on safety factors in order to avoid failure due to concentration stress^[23,24].

Many efforts have been made to calculate the stress in a strip containing a central circular hole when subjected to

tension. The analysis showed that there is a high concentration of stress at both edges of hole parallel to the direction of loading. When the size of the hole is small compared to the width of strip, it is possible to calculate the value of stress at any point located at a distance (a) from the center of the hole, shown in Fig.(2), by ^[24] :

$$\sigma_{\max} = \frac{\sigma}{2} \left[2 + \left(\frac{d^2}{4a^2} \right) + \left(\frac{3}{16} \right) \left(\frac{d^4}{a^4} \right) \right] \dots(4)$$

If σ indicates the stress at both ends of the strip $d =$ hole diameter ($2r$ twice the radius of the hole), therefore the maximum value of stress at the edges of hole parallel to the axis of loading i.e. when $r = a$ is equal ($\sigma_{\max} = 3\sigma$): this value decreases when moving away from the edges ^[22]. Stress components were calculated using the elastic analysis; these are the radial stress (σ_r) and tangential stress (σ_θ), and shear stress (σ_s), which are calculated at a distance (a) from the center of a circular hole of radius (r) in an infinite strip subjected to tension, as shown in Fig.(2) as ^[24]:

$$\sigma_r = \frac{\sigma}{2} \left[1 - \left(\frac{r^2}{a^2} \right) \right] + \dots(5)$$

$$\left(\frac{\sigma}{2} \right) \left[1 + \left(\frac{3r^4}{a^4} \right) - \left(\frac{4r^2}{a^2} \right) \right] \cos 2\theta$$

$$\sigma_\theta = \frac{\sigma}{2} \left[1 + \left(\frac{r^2}{a^2} \right) \right] - \dots(6)$$

$$\left(\frac{\sigma}{2} \right) \left[1 + \left(\frac{3r^4}{a^4} \right) \right] \cos 2\theta$$

$$\sigma_s = -\frac{\sigma}{2} \left[1 - \left(\frac{3r^4}{a^4} \right) + 2 \left(\frac{r^2}{a^2} \right) \right] \sin 2\theta \quad (7)$$

When ($a = r$) and the value of the angle ($\theta^0 = 0^0, 180^0$), the tangential

stress at the edges of the hole, the upper and the lower (A,B), will be: $\sigma_\theta = -\sigma$. Also, if ($a = r$) and the value of the angle ($\theta^0 = 90^0, 270^0$), the tangential stress at both edges of the hole at the side(D,C), will be: $\sigma_\theta = 3\sigma = \sigma_{\max}$.

Numerical Work

The numerical work was all done using the FEM-based commercial well-known software ANSYS. A short review of the method as well as the equations employed in a classical run by the software was attached in the Appendix.

Four types of cutout were selected throughout the program of numerical work. These are circular, triangular, square and pentagonal cutouts. In all cases a flat plate, having length of ($2L$) = 100 mm, width of ($2B$) = 100mm, thickness of ($t = 1$ mm) and hole radius of ($R = 2$ mm), was subjected to pure tension, see Fig.(3). Typical values for the mechanical properties of an isotropic material of the plate were chosen, namely $E = 200$ GPa, $\nu = 0.3$.

It should be noted that the element type employed in the present work was PLANE145 which may be used as a plane stress element. This element is a triangular, six node element having two degrees of freedom at each node (linear displacements) ^[25].

As usual, advantage was taken of symmetry so that more elements could be used especially at the cutout corner where highly-localized stress is expected. Convergence tests were also made for optimizing, the various types of meshes.

Total number of 174 runs was exacted in the present work.

In order to facilitate presentation of the present work, the various parameters that affect the stress concentration factor were grouped as follows:

Group 1: deals with the effect of cutout location along an axis (x)

displaced by an angle (θ) from the axis of loading, see Fig.(3). Three values of (θ) were examined, namely ($0^\circ, 45^\circ$ and 90°).

Group 2: deals with the effect of angle of rotation (θ) of a central cutout with respect to the axis of loading, see Fig.(3) . Values of (θ) up to 90° were examined.

Group 3: deals with the effect of corner sharpness of a central and non-rotated cutout, see Fig.(4). Values of (r_c/R) as high as (1), were examined.

Group 4: deals with the effect of the plate thickness. Values of (t/B) in the range (0.01 – 0.03) were examined.

Results and Discussion

As mentioned earlier, four groups of parameters were examined to reveal its effect on the stress concentration factor in a uni-axially – tensioned plate with different types of cutout. Therefore, the results found and discussed, were grouped in the same manner, as follows:

Group1: The effect of cutout location (x/l), along an axis (x) displaced by an angle (θ) of ($0^\circ, 45^\circ$ and 90°), is shown in Figs.(5, 6 and 7) respectively. In these figures, the (SCF) increases as the number of sides in a cutout decreases, i.e as a cutout is changed from circular to pentagonal, to square and to triangular cutout. Thus (SCF) of a hexagonal cutout will be less than a pentagonal one, but still it is higher than a circular cutout.

This result is seen to confirm the work by Rezaeepazhand and Jafari ^[5] and Rajab ^[6] who used a hexagonal cutout in addition to the presently used types of cutouts. Moreover, this result validates the results obtained using the present numerical work. It should be noted that, in general, there is an agreement among many researchers that any type of cutout other than circular will be accompanied by an increase in the value of SCF. The reason is

normally attributed to the presence of sharp corners in the cutouts other than circular ones.

Moreover, these figures show almost a general trend of decreasing in (SCF) values with the cutout location up to ($x/l = 0.4$) above which the (SCF) restores its value at ($x/l = 0.7$). The somewhat irregular changes in (SCF) values are attributed to the Saint Venant's principle which states that there are considerable changes in the state of stress near the loading points. The most interesting result displayed by these figures , that the presence of a circular hole at locations, other than the center of plate, would be beneficial especially at locations near $x/l = 0.15$.

Group 2: The effect of rotation angle (θ) of a central cutout is shown in Fig.(8). In this figure, it is well apparent that the (SCF) for a given type of cutout is fluctuating between minimum and maximum values at equal intervals of rotation angle. Thus, for the triangular cutout, the (SCF) fluctuates between 4.75 to 5.25 every 30° of rotation; for the square cutout, the (SCF) fluctuates between 3.75 to 4.25 every 45° of rotation; for the pentagonal cutout, the (SCF) fluctuates between 3.65 to 3.85 every 36° of rotation. As the rule, the maximum value of (SCF) for a given cutout occurs at a corner when an axis, perpendicular to the axis of loading, bisects the angle of that corner.

A relevant work was conducted by Rajab ^[6] who found similar intervals during which the SCF value is fluctuating. Besides, it was concluded that down to a value of $SCF = 2.88$ would be attained when rotating a square cutout through 10° ; a result which is not the case in the present work which reports an optimum angle of 30° corresponding to a value of $SCF = 3.75$.

A less relevant study by Rezaeepazhand and Jafari ^[5] , who used

anisotropic material, found optimum values of angle of rotation of both the cutout orientation and loading axis.

Group 3: The effect of corner radius (r_c/R) is shown in Fig.(9), where the value of (SCF) for a given cutout decreases nearly at constant rate as the corners are being rounded or the radius of curvature is increased. When r_c approaches R the cutouts change in shape to different shapes close to a circular one. To mention, in particular, the pentagonal cutout is reshaped to a circular one where the (SCF) approaches the well known value of (3).

This result reflects the common reasoning that the rounding of sharp corners minimizes the stress concentration. Moreover, a larger radius of corner will further minimize the stress concentration.

It should be mentioned herein that a value of $SCF = 2.6$ was reported by Rezaeepazhand and Jafari^[5] when using a square cutout of rounded corners if the cutout is rotated through an angle of 45° . This result seems to be questionable in view of the present results in which neither rotating the cutout nor the rounding of corners succeeds in lowering the value of SCF below a value of $SCF = 3$.

Group 4: The effect of thickness of the plate is shown in Fig.(10). The values of thickness were intentionally selected in the range where the plane stress state is maintained. It is interesting to note that the values of (SCF), decreases as the thickness is increased; a result which is missed in assumptions made by many researchers.

Should the thickness increased beyond those of Fig.(10), a transfer from plane stress to a plane strain state may occur. The transition range of thickness so obtained needs extensive work in future.

Conclusions

To summarize the main conclusions drawn out of the present work:

1. The location of a cutout at points other than the center seems to decrease the values of (SCF) in a manner dictated by restriction due to Saint Venant's principle.
2. Maximum value of (SCF) at a corner is attained, for a given type of cutouts, when an axis, perpendicular to the axis of loading, bisects the angle of that corner.
3. Increasing the radius of bluntness decreases the values of (SCF).
4. The thickness of the plate does have an effect on the values of (SCF). Lower values of (SCF) are attained upon increasing the thickness of a plate.

References

1. L.J. Monahan, P.J. Nemergut, G.E. Maddux, Natural frequencies and mode shapes of plates with interior cut-outs, *The Shock and Vibration Bulletin*, V.41, N.3, 1970.
2. P. Paramasivam, Free vibration of square plates with square opening, *Journal of Sound and Vibration*, V.30, N.2, 1973.
3. G. Aksu, R. Ali, Determination of dynamic characteristics of rectangular plates with cut-outs, using a finite difference formulation, *Journal of Sound and Vibration*, V.44, N.1, 1976.
4. A. Rajamani, R. Prabhakaran, Dynamic response of composite plates with cut-outs. Part I: Simply – supported plates. *Journal of Sound and Vibration*, V.54, N.4, 1977.
5. Rezaeepazhand J, Jafari M. Stress concentration in metallic plates with special cutout. *Int. J. Mech. Sci.* V.52, N.1, 2010.
6. Rajab M. A., Study on static and fatigue performance of die steel with multiple stress concentrators, Ph.D thesis, University of Technology, 1999.

7. K. Y. Lam, K.C. Hung, S.T. Chow, Vibration analysis of plates with cut-outs by the modified Rayleigh – Ritz method. *Applied Acoustics* , V.28, N.1 ,1989
8. K. Y. Lam, K.C. Hung, Vibration study on plates with stiffened opening using orthogonal polynomials and partitioning method, , *Computers and Structures*, V.37, N.3 ,1990.
9. R.B. Bhat, Natural frequencies of rectangular plates using characteristic orthogonal polynomials in Rayleigh – Ritz method, *Journal of Sound and Vibration* , V.102, N.4 ,1985.
10. R.B. Bhat, Numerical experiments on the determination of natural frequencies of transverse vibrations of rectangular plates of nonuniform thickness, *Journal of Sound and Vibration* , V.138, N.2 ,1990.
11. P.A.A. Laura, E. Romanelli, R.E. Rossi, Transverse vibrations of simply-supported rectangular plates with rectangular cut-outs, *Journal of Sound and Vibration*,V.202, N.2,1997
12. T. Sakiyama, M.Huang, H. Matsuda, C.Mrita, Free vibration of orthotropic square plates with a square hole. *Journal of Sound and Vibration* , V.259, N.1, 2003.
13. S. Takahashi, Vibration of rectangular plates with circular holes. *Bulletin of JSME* ,V.1, N.4,1958.
14. Theocaris PS,. Stress distributions and intensities at corners of equilateral triangular hole.*Journal of Fracture* , V.31, N.2 , 1986.
15. Theocaris PS.Petrou L From the rectangular hole to ideal crack. *International journal of solids and structures* , V.25, N.3, 1989.
16. Lasko GV, Deryugin YY, Schmauder S, Saraev D. Determination of stresses near multiple pores and rigid inclusion by relaxation elements. *Theoretical and Applied Fracture Mechanics* .V.34, N.1, 2000.
17. Paik Jeom Kee. Ultimate strength of perforated steel plates under edge shear loading. *Thin – Walled Structures*, V.45, N.3, 2007.
18. Ulz M.H, Semercigil S.E. ,Vibration control for plate- like structures using strategic cut-outs. *Journal of Sound and Vibration* , V.309, N.1-2 , 2008.
19. Dai L, Guo W, Wang X. Stress concentration at an elliptic hole in transversely isotropic piezoelectric solids. *Int. journal of solids and structures*, V.43, N.6 , 2006.
20. Rezaeepazhand J, Jafari M. Stress analysis of perforated composite plates. *Composite Structures* , V.71, N.3-4 , 2005.
21. S.P. Timoshenko and D.H. Young, *Elements of strength of materials*. Third Edition P.47-331.
22. M. Hamada, I. Mizushima and T.Masuda . A Numerical Method for Stress concentration with problems of infinity plates with many circular holes subjected to uniaxial tension. *Journal of Engineering Materials Technology*, January 1974, P.65-70.
23. George E. Dieter. *Mechanical Metallurgy*. Second edition, McGRAW-Hill Series Materials Science Engineering , P.66.
24. E.J. Hearn. *Mechanics of materials*. Second edition, Pergamon Press Headington Hill, Oxford O_{x3} OBW, England, 1985, P.804.
25. ANSYS, Inc. *Theory Reference*.

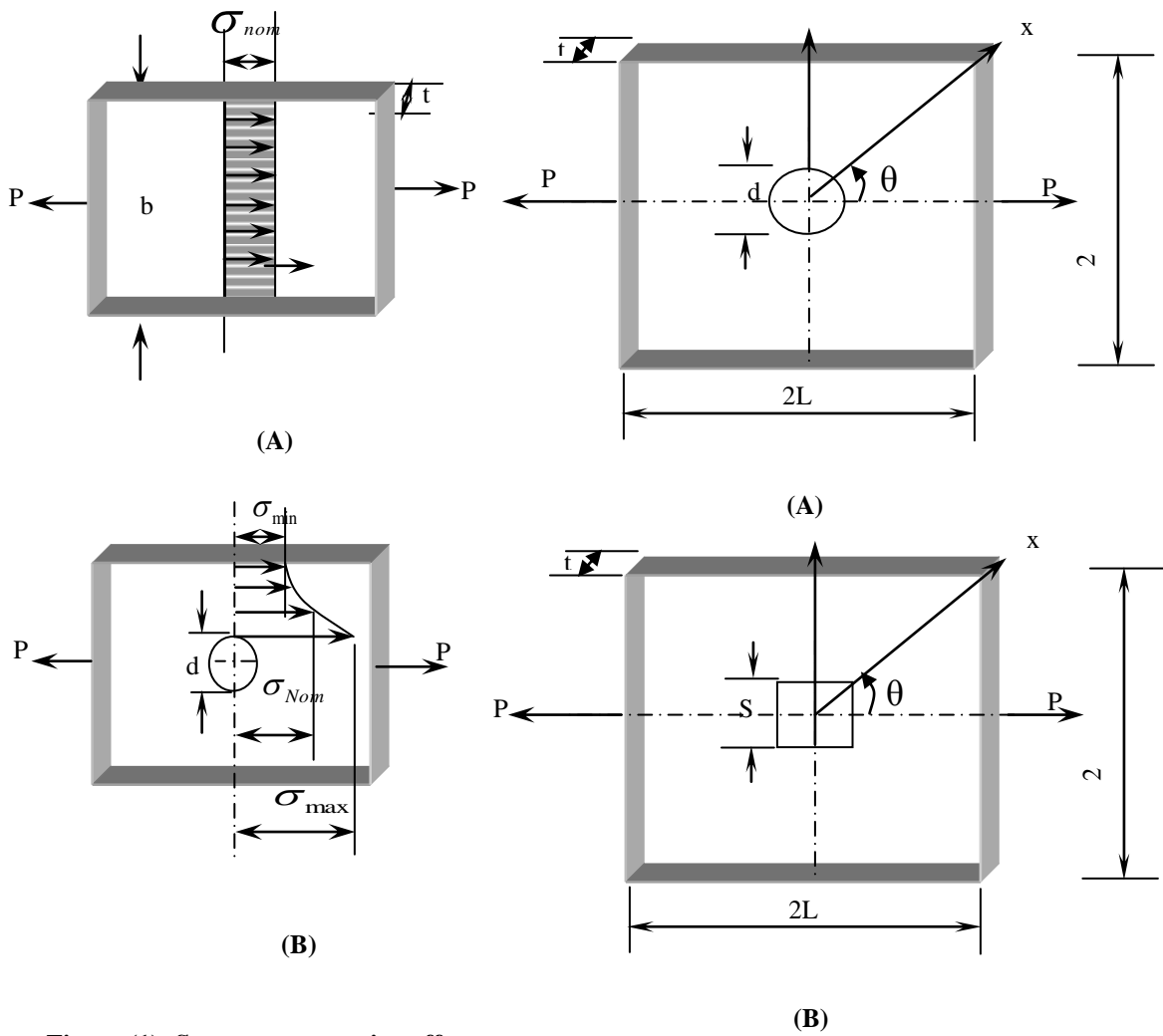


Figure (1): Stress concentration effect of a hole [24]

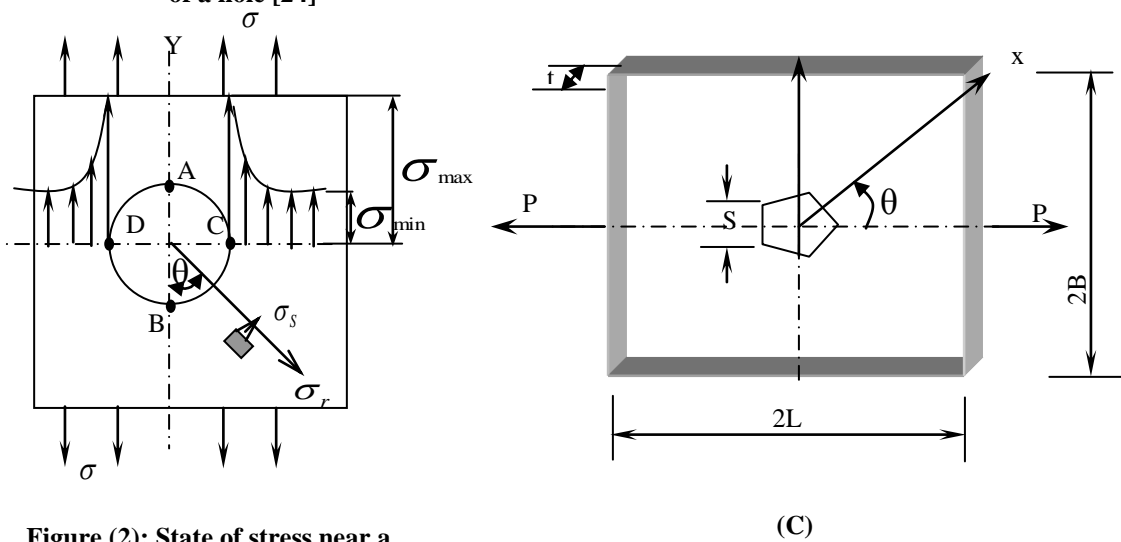


Figure (2): State of stress near a hole[24].

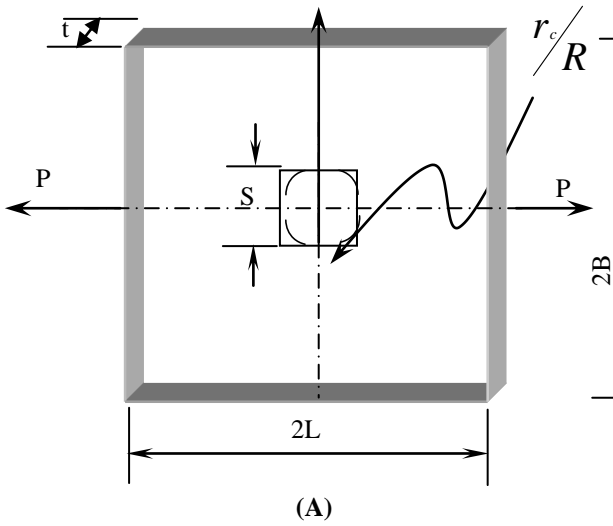


Figure (3): Types of cutouts with sharp corners.

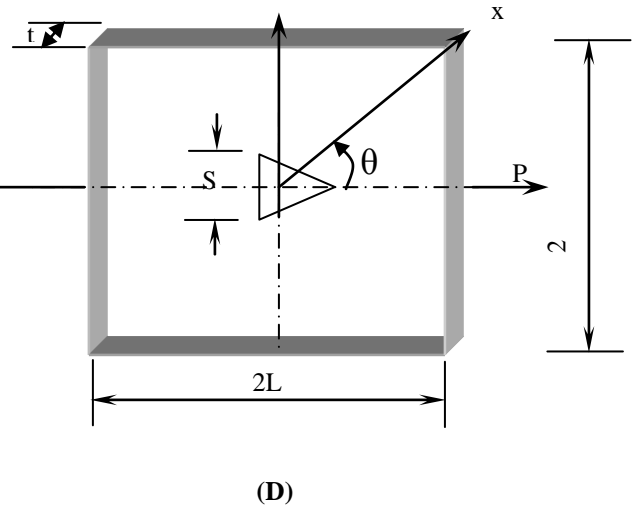
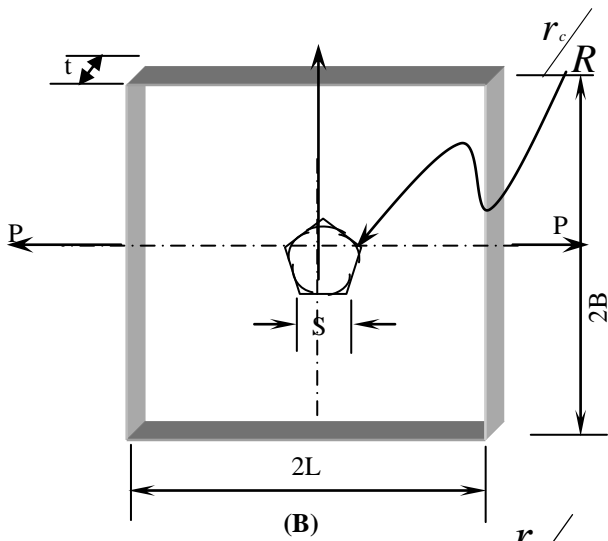


Figure (4): Types of cutouts with rounded corners.



(B)

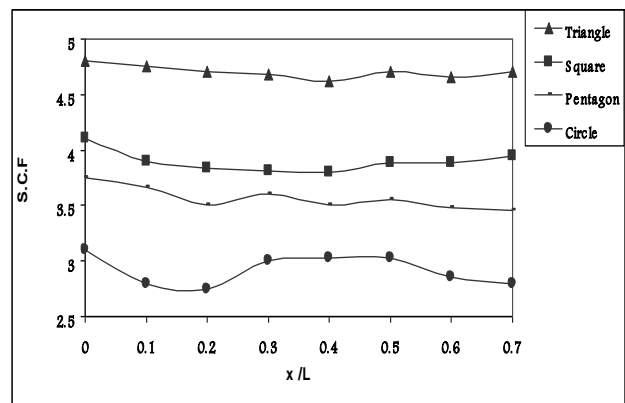
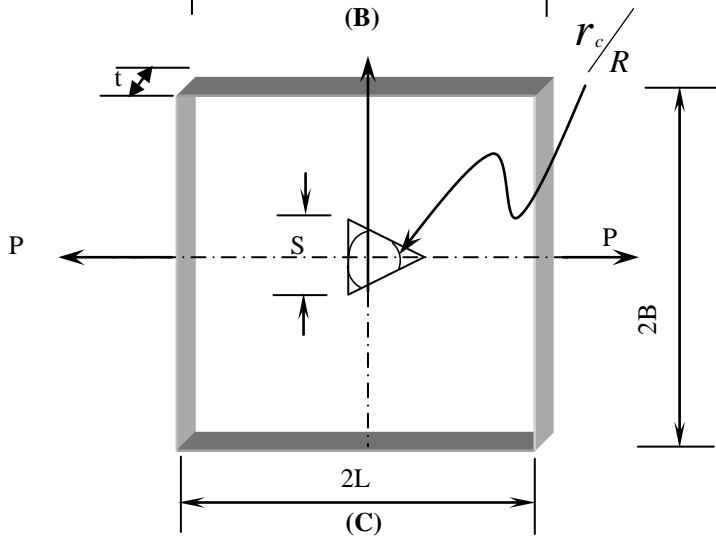


Figure (5): Effect of location of cutout on the S.C.F at $\theta = 0^\circ$.



(C)

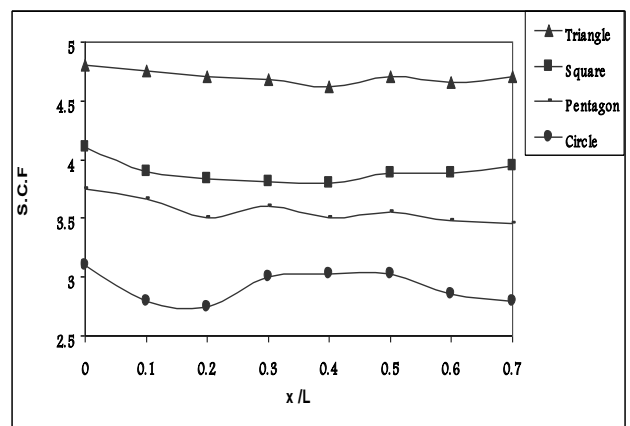


Figure (6): Effect of location of cutout on the S.C.F at $\theta = 45^\circ$.

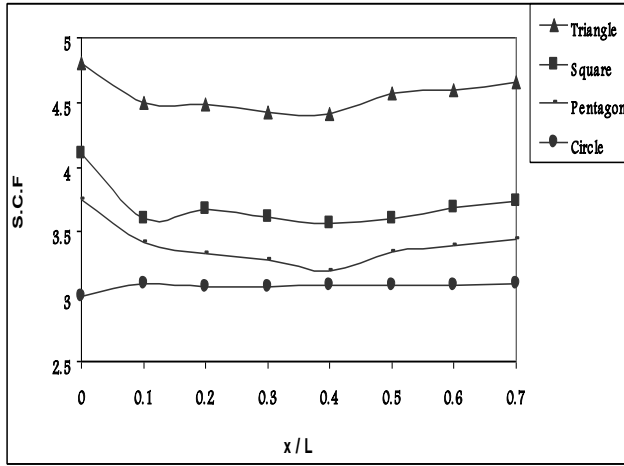


Figure (7): Effect of location of cutout on the S.C.F at $\theta = 90^\circ$.

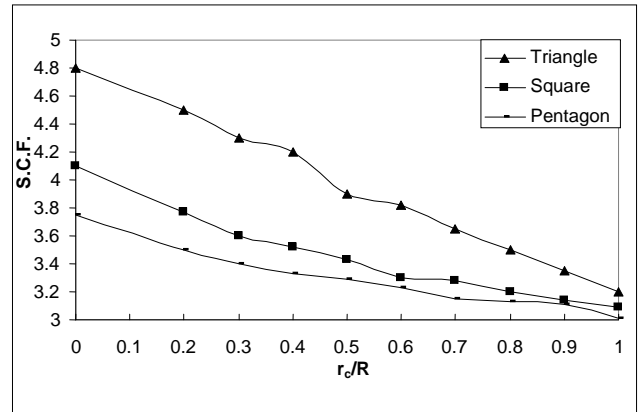


Fig.(9): Effect of sharpness of corner cutout on the S.C.F.

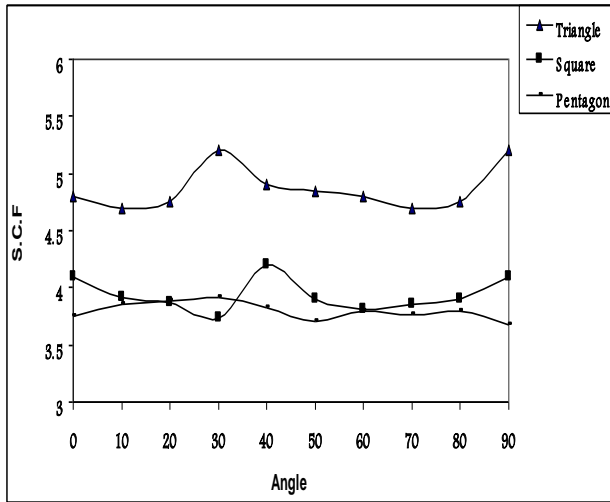


Figure (8): Effect of angle rotation of cutout on the S.C.F.

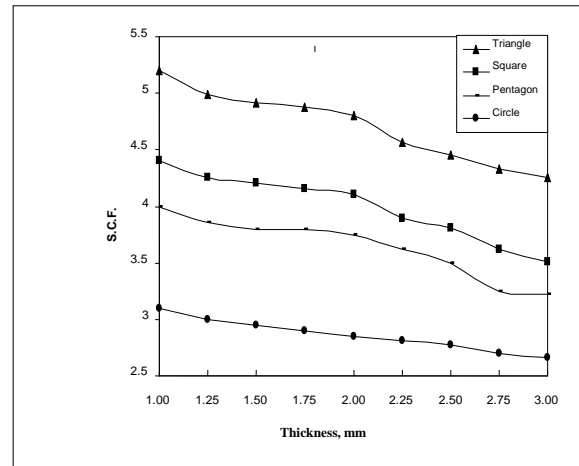


Fig.(10): Effect of thickness on the S.C.F.

Appendix^[25]

Introduction

The F.E.M. is a numerical technique in which the governing equations are represented in matrix form and as such are well suited to solution by digital computer. The solution region is idealized as an assemblage of small sub-regions called finite elements. When applied to the analysis of a solid the idealization becomes an assemblage of a discrete number of elements each with a limited or FINITE number of degrees of freedom (D.O.F.). The ELEMENT is the basic "building unit", with a predetermined number of D.O.F.

Elements are considered to be connected at discrete joints known as nodes. Implicit with each element type is the nodal force-displacement relationship, namely the element stiffness property. Analysis requires the assembly and solution of a set of simultaneous equations, to provide the displacements for every node in the model. Once the displacement field is determined, the strain and hence stresses can be derived, using the strain-displacement and stress-strain relations, respectively.

F.E.M. solution of plane stress problem:

The three-nodded triangles, shown in Fig. A, has been chosen herein, to illustrate the general procedure since it provides the simplest two-dimensions element for linear plane-stress analysis.

Formulation of element matrices and vectors:

Each node of the element, shown in Fig. A, is assumed to have two D.O.F., namely u and v displacements in the x and y-direction, respectively.

Interpolation polynomial:

They are functions that are used to represent the behavior of the solution within an element. In the present

example the assumed interpolation polynomial with describe the displacements, and hence called the "displacement function".

Both u and v displacements are assumed to vary linearly in the x and y directions, respectively, i.e:

$$u(x,y) = \alpha_1 + \alpha_2 x + \alpha_3 y$$

$$v(x,y) = \alpha_4 + \alpha_5 x + \alpha_6 y$$

or, in matrix form:

$$\begin{bmatrix} u \\ v \end{bmatrix} = \begin{bmatrix} 1 & x & y & 0 & 0 & 0 \\ 0 & 0 & 0 & 1 & x & y \end{bmatrix} \begin{bmatrix} \alpha_1 \\ \alpha_2 \\ \alpha_3 \\ \alpha_4 \\ \alpha_5 \\ \alpha_6 \end{bmatrix} \dots(A1)$$

Substituting boundary conditions at x = x_i and y = y_i, u = u_i and v = v_i at x = x_j and y = y_j, u = u_j and v = v_j at x = x_k and y = y_k, u = u_k and v = v_k gives:

$$\begin{bmatrix} u_i \\ u_j \\ u_k \\ v_i \\ v_j \\ v_k \end{bmatrix} = \begin{bmatrix} 1 & x_i & y_i & 0 & 0 & 0 \\ 1 & x_j & y_j & 0 & 0 & 0 \\ 1 & x_k & y_k & 0 & 0 & 0 \\ 0 & 0 & 0 & 1 & x_i & y_i \\ 0 & 0 & 0 & 1 & x_j & y_j \\ 0 & 0 & 0 & 1 & x_k & y_k \end{bmatrix} \begin{bmatrix} \alpha_1 \\ \alpha_2 \\ \alpha_3 \\ \alpha_4 \\ \alpha_5 \\ \alpha_6 \end{bmatrix}$$

Or more concisely:

$$\{p\} = [A] \{\alpha\} \dots(A2)$$

Formulation of element stress-strain matrix:

The stress-displacement relations for a plane stress condition are:

$$\begin{aligned} \epsilon_{xx} &= \frac{\partial u}{\partial x}, & \epsilon_{yy} &= \frac{\partial u}{\partial y}, \\ \epsilon_{xy} &= \frac{\partial u}{\partial y} + \frac{\partial u}{\partial x}, \dots(A3) \end{aligned}$$

Where ϵ_{xx} , ϵ_{yy} and ϵ_{xy} are respectively, the direct strains parallel to

x and y axes and the shear strain in the xy plane.

In matrix form:

$$\{\varepsilon\} = \begin{bmatrix} \varepsilon_{xx} \\ \varepsilon_{yy} \\ \varepsilon_{xy} \end{bmatrix} = \begin{bmatrix} \frac{\partial}{\partial x} & 0 \\ 0 & \frac{\partial}{\partial y} \\ \frac{\partial}{\partial y} & \frac{\partial}{\partial x} \end{bmatrix} \begin{bmatrix} u \\ v \end{bmatrix} \dots\dots\dots(\text{A4})$$

Substituting from Eq. A1 gives:

$$\{\varepsilon\} = \begin{bmatrix} 0 & 1 & 0 & 0 & 0 & 0 \\ 0 & 0 & 0 & 0 & 0 & 1 \\ 0 & 0 & 1 & 0 & 1 & 0 \end{bmatrix} \begin{bmatrix} \alpha_1 \\ \alpha_2 \\ \alpha_3 \\ \alpha_4 \\ \alpha_5 \\ \alpha_6 \end{bmatrix}$$

Which is of the form:

$$\{\varepsilon\} = [B] \{\alpha\} \dots\dots\dots(\text{A5})$$

For plane stress conditions ($\sigma_{zz} = \sigma_{xz} = \sigma_{xy} = 0$) and isotropic material, the stress-strain relations in matrix form are:

$$\{\sigma\} = \begin{bmatrix} \sigma_{xx} \\ \sigma_{yy} \\ \sigma_{xy} \end{bmatrix} = \frac{E}{1-\nu^2} \begin{bmatrix} 1 & \nu & 0 \\ \nu & 1 & 0 \\ 0 & 0 & \frac{1-\nu}{2} \end{bmatrix} \{\varepsilon\}$$

i.e:

$$\{\sigma\} = [D] \{\varepsilon\} \dots\dots\dots(\text{A6})$$

Where σ_{xx} , σ_{yy} and σ_{xy} are respectively, the direct stresses parallel to x and y axes and the shear stress in the xy plane, and [D] is known as the " elasticity matrix".

Formulation of element stiffness matrix:

Equating the total, internal and external, virtual work yield the generalized coordinate stiffness:

$$[k] = \int_{vol} [B^T] [D] [B] dv \dots\dots\dots(\text{A7})$$

Since both matrices [B] and [D] are independent of the x and y coordinates, hence:

$$[k] = at [B^T][D][B] \dots\dots\dots(\text{A8})$$

Where (a) is the area of the element and (t) is the element thickness (assumed to be constant).

Assembly of elements:

The assembly process to obtain the structure stiffness matrix, [k] can be written as:

$$[k] = \sum_{i=1}^m [k_i] \dots\dots\dots(\text{A9})$$

Where $[k_i]$ is the stiffness matrix of the ith element and m is the total number of elements in the assemblage.

In the same manner, the structure load vectors {p} are assembled, i.e:

$$\{p\} = \sum_{i=1}^m \{p_i\} \dots\dots\dots(\text{A10})$$

Solution of the structure equilibrium equations:

Once the boundary conditions have been applied, the system of equs.:

$$\{P\} = [k] \{p\}$$

Can be solved using direct or iterative methods.

Computation of element results:

The solution of the final equations will provide the vector of global nodal displacements $\{p_a\}$ for the enter structure.

Element stresses can now be expressed in terms of nodal displacements by use Eqs. A6,A5 and A2. i.e.:

$$\{\sigma\} = [D][B][A^{-1}]\{P_e\}$$

Or, more fully,

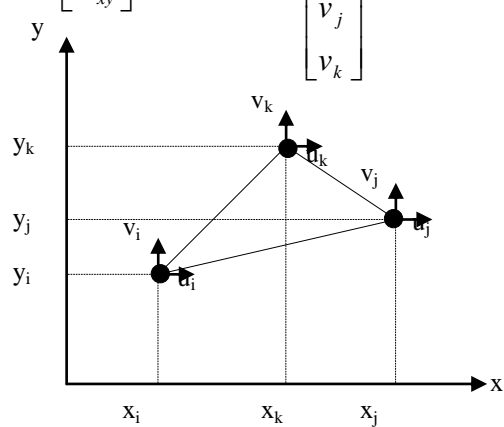
$$\begin{bmatrix} \sigma_{xx} \\ \sigma_{yy} \\ \sigma_{xy} \end{bmatrix} = [D][B][A^{-1}] \begin{bmatrix} u_i \\ u_j \\ u_k \\ v_i \\ v_j \\ v_k \end{bmatrix}$$


Figure A: Three-noded triangular plane element [25].